Original Article

OPEN

# Morphometric analysis of small arteries in the human retina using adaptive optics imaging: relationship with blood pressure and focal vascular changes

**Edouard Koch[a], David Rosenbaum[b], Aurélie Brolly[a], José-Alain Sahel[a], Philippe Chaumet-Riffaud[a,c], Xavier Girerd[b], Florence Rossant[d], and Michel Paques[a]**

**Objectives:** The wall-to-lumen ratio (WLR) of retinal arteries is a recognized surrogate of end-organ damage due to aging and/or arterial hypertension. However, parietal morphometry remains difficult to assess *in vivo*. Recently, it was shown that adaptive optics retinal imaging can resolve parietal structures of retinal arterioles in humans *in vivo*. Here, using adaptive optics retinal imaging, we investigated the variations of parietal thickness of small retinal arteries with blood pressure and focal vascular damage.

**Methods:** Adaptive optics imaging of the superotemporal retinal artery was done in 49 treatment-naive individuals [mean age (±SD) 44.9 years (±14); mean systolic pressure 132 mmHg (±22)]. Semi-automated segmentation allowed extracting parietal thickness and lumen diameter. In a distinct cohort, adaptive optics images of arteriovenous nicking (AVN; $n = 12$) and focal arteriolar narrowing (FAN; $n = 10$) were also analyzed qualitatively and quantitatively.

**Results:** In the cohort of treatment-naive individuals, by multiple regression taking into account age, body mass index, mean, systolic, diastolic and pulse blood pressure, the WLR was found positively correlated to mean blood pressure and age which in combination accounted for 43% of the variability of WLR. In the cohort of patients with focal vascular damage, neither FANs or AVNs showed evidence of parietal growth; instead, at sites of FANs, decreased outer diameter suggestive of vasoconstriction was consistently found, while at sites of AVNs venous narrowing could be seen in the absence of arteriovenous contact.

**Conclusion:** High resolution imaging of retinal vessels by adaptive optics allows quantitative microvascular phenotyping, which may contribute to a better understanding and management of hypertensive retinopathy.

**Keywords:** adaptive optics, arterial hypertension, retina, small vessels, wall-to-lumen ratio

**Abbreviations:** AO, adaptive optics; AVN, arteriovenous nicking; FAN, focal arteriolar narrowing; SDLF, scanning laser Doppler flowmetry; WCSA, wall cross-sectional area; WLR, wall-to-lumen ratio

## INTRODUCTION

Arterial hypertension and aging affects the structure of small arteries. An increase of the wall-to-lumen ratio (WLR) is a hallmark of hypertensive microangiopathy and is predictive of end-organ damage [1–4]. The prevalent physiopathological concept of such parietal thickening postulates that a rise in blood pressure stimulates myogenic vasoconstriction, which tends to normalize parietal tension [5,6], without significant modification of the parietal components (a process called eutrophic remodelling). However, there is currently a lack of clinically pertinent methods for measuring parietal thickness. Myographic and histological investigations are indeed not applicable in clinical routine. Conversely, the retina being an easily accessible part of the microcirculation, in-vivo evaluation of the microvascular consequences of arterial hypertension can be done on fundus photographs. The most prevalent lesions of hypertensive retinopathy are diffuse narrowing of arterioles and focal lesions such as focal arteriolar narrowing (FAN) and arteriovenous nicking (AVN). Several large-scale epidemiological studies reported that the severity and/or incidence of these signs correlate with past and incident arterial pressure [7–10] and with end-organ damage [11–14]. The clinical evaluation of hypertensive retinopathy is however limited by the fact that fundus photographs or fluorescein angiography do not enable visualizing the arteriolar wall. An indirect measure of the arteriolar wall thickness based on the differential analysis of

Journal of Hypertension 2014, 32:890–898

[a]Clinical Investigation Center 503, Centre Hospitalier National des Quinze-Vingts, INSERM and Université Pierre et Marie Curie-Paris6, [b]Preventive Cardiovascular Unit, Institute of Cardiometabolism and Nutrition, Pitié-Salpêtrière Hospital, Assistance Publique-Hôpitaux de Paris, [c]Université Paris-Sud, Hôpital Bicêtre, Assistance Publique-Hôpitaux de Paris, and [d]Institut Supérieur d'Electronique de Paris, Paris, France

Correspondence to Michel Paques, MD, PhD, Clinical Investigation Center 503, Centre Hospitalier National des Quinze-Vingts, 28 rue de Charenton 75012 Paris, France. Tel: +33 1 40 02 14 15; fax: +33 1 40 02 14 99; e-mail: michel.paques@gmail.com

**Received** 29 July 2013 **Revised** 28 November 2013 **Accepted** 28 November 2013



DOI:10.1097/HJH.0000000000000095

laser Doppler and reflectance imaging (scanning laser Doppler flowmetry, SDLF) of the retina has been proposed [15–17]. However, this technique has a relatively limited spatial resolution, which impairs in particular the analysis of focal lesions.

Adaptive optics is an opto-electronic technology that improves the resolution of fundus images. Current adaptive optics-based fundus cameras enable visualization of microstructures such as photoreceptors [18], capillaries [19] or vascular wall [20] noninvasively in humans. Here, following our pilot study [21], we evaluated a novel approach of microvascular morphometry using adaptive optics imaging, which may ultimately help to better understand and manage hypertensive microangiopathy.

## METHODS

This clinical study was carried out according to the principles outlined in the Declaration of Helsinki. Approval of the Ethics Committee of the Saint-Antoine hospital (Paris, France) was obtained. Patients older than 18 years with clear ocular media and no ocular or systemic diseases apart from arterial hypertension were considered eligible. Patients were recruited at the Preventive Cardiovascular Unit of the Pitié-Salpêtrière Hospital. Other patients with AVNs and/or FANs were also recruited at the Quinze-Vingts Hospital. Each patient received full oral and written information and gave written consent prior to inclusion.

### Adaptive optics retinal imaging

Retinal imaging was performed at the Clinical Investigation Center of the Quinze-Vingts Hospital. En face adaptive optics fundus images were obtained using a commercially available flood-illumination adaptive optics retinal camera (rtx1; Imagine Eyes, Orsay, France). Briefly, the rtx1 camera measures and corrects wavefront aberrations with a 750 nm super luminescent diode source and an adaptive optics system operating in a closed loop. A $4 \times 4$ fundus area (i.e. approximately $1.2 \times 1.2$ mm in emmetropic eyes) is illuminated at 840 nm by a temporally low coherent light-emitting diode flashed flood source, and a stack of 40 fundus images is acquired in 4 s by a charge-coupled device camera.

Most examinations were done without pupil dilation; if needed, pupil dilation was obtained with topical tropicamide (Novartis, France). After a 10-min rest during which the examination was explained, the patient was installed on the chin rest. The measured refraction was integrated into the camera. The live video image of the pupil allowed alignment with the incident light; the live display of adaptive optics-corrected fundus image allowed brightness, contrast and focus to be adjusted. Gaze was oriented by an internal or external target in order to capture the region of interest. The reference site was a segment of the superotemporal artery of the right eye, at least 250 μm long with an inner diameter of at least 50 μm, devoid of bifurcations, one disc diameter from the disc (see example in Fig. 1a). Blood pressure (BP) was measured in the sitting position simultaneously to adaptive optics image acquisition using an automated oscillometric device using an arm cuff (VS800, Mindray Corporation; Shenzhen, China). Two measures of BP were taken before starting the acquisition process; then one BP measurement was then performed during each image acquisition.

To identify the systolic pulse and delete the corresponding images, real-time videos were generated from each stack using a customized plugin developed under ImageJ software (see examples in supplementary video 1 and 2, http://links.lww.com/HJH/A317, http://links.lww.com/HJH/A318 [adaptive optics videofundoscopy of the superotemporal artery and vein in the right eye of a 26 years old man (same patient as in figure 1). Note the visibility of the arterial wall but not of the venous wall, and the systolic curving of the arteriole (Quicktime video; image width 1.2mm; 40 frames, 10 fps); adaptive optics videofundoscopy of the superotemporal artery in the right eye of a 40 years old healthy woman (Quicktime video; image width 1.2 mm; 40 frames, 10 fps). ]). Then, the diastolic images were averaged to increase the signal-to-noise ratio (Fig. 1b; see ref.[22] for supplementary details, http://links.lww. com/HJH/A316).

### Image analysis

Averaged adaptive optics images were semi-automatically segmented using a custom software running under Matlab (Mathworks, Natick, Massachussetts, USA). Briefly, the processed adaptive optics images, after being encoded on 8 bits, were first enhanced by applying a median filter followed by a nonlinear diffusion filter [23]. Such filters allow smoothing the blood vessels while preserving the contrast along their edges. The first step of the segmentation is based on the enhancement of the axial reflection and the detection of the darkest regions, by applying respectively morphological operations and k-means classification. Both are then fused in order to select the axial reflection of the vessel and compute a binary mask of the vessel. The second step of the segmentation process aims at extracting the borders of the vessel. Each side is approximated by a curve parallel to the regularized skeleton of its axial reflection [24,25]. The mean distance between a side contour and the central reflection line is deduced from the binary mask and the gradient image; it is adjusted so that the obtained curve is placed as near as possible to the internal side of the parietal structure. This segmentation is then refined by applying a parametric active contour with a parallelism constraint [26]. In this model, a curve evolves towards the higher gradients of the image (the edges) while maintaining locally an approximate parallelism with the reference line (the axial reflection), which improves robustness regarding image noise. The algorithm is applied twice in order to segment the internal limits of the vessel lumen. Then, the initialization is automatically modified in order to segment the outer limits. Thus, a complete segmentation of the arterial wall is obtained (Fig. 1b), with a point-by-point correspondence between opposite sides of the vessel. The whole segmentation process is under human supervision. Graphic representations of morphometric parameters along a given vessel segment (termed here morphograms; Fig. 1c) were generated. The ratio of total parietal thickness (P) over the lumen diameter (D) averaged over 250 μm defined the WLR. The cross-sectional surface of the vessel wall, averaged over 250 μm, defined the wall cross-sectional area (WCSA). All measures were done in a masked fashion.

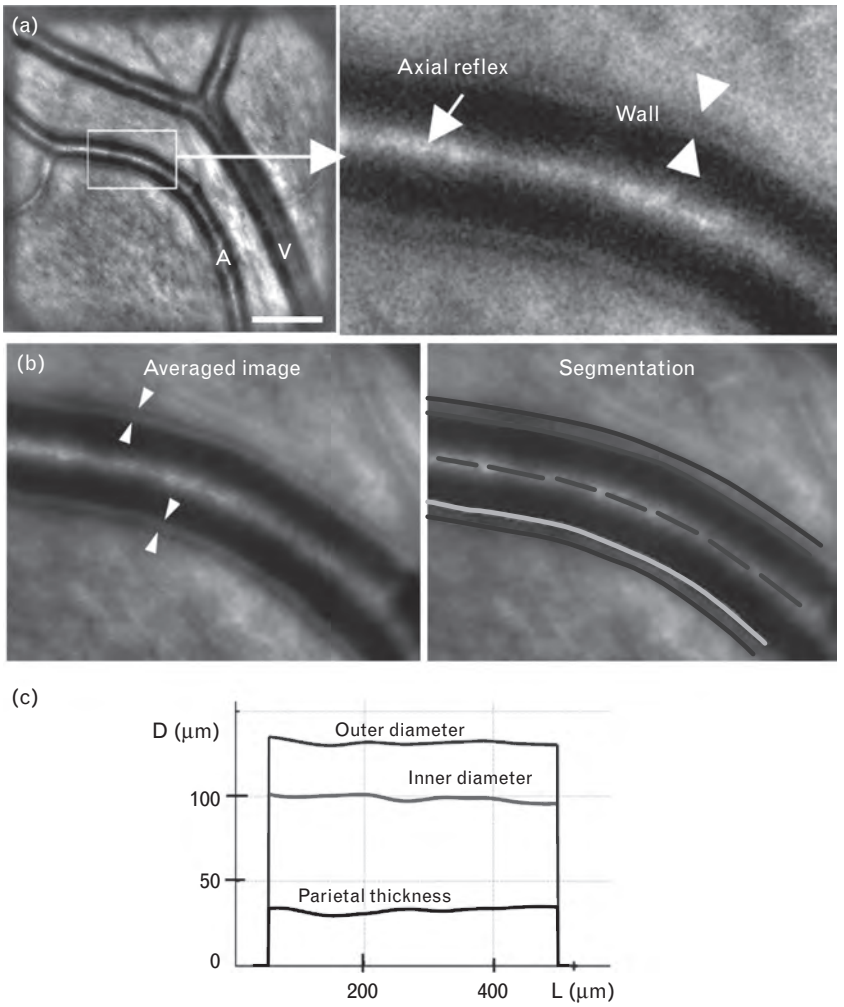


**FIGURE 1** Adaptive optics (AO) imaging and segmentation of a retinal arteriole (same patient as in supplementary video 1, http://links.lww.com/HJH/A317). (a) Single videoframe (right panel: magnification). Note that parietal structures (between arrowheads in magnification) can be seen (A: arteriole, V: venule; bar, 250 μm). (b) Image averaging and segmentation. (c) Morphogram of the segmented vessel (D: diameter; L: length).

## Statistics

Descriptive statistics of quantitative and ordinal variables and analysis of normality of distribution were performed. The means of quantitative variables between two groups were compared using the parametric *t* test for independent samples. The homogeneity of variance was checked using Levene's test. The relationship between two variables (interval data) was investigated by calculating Pearson's correlation coefficient. In some cases, Kendall's correlation values were also calculated. To test intra-observer and inter-observer reproducibility, three consecutive measures of WLR and lumen diameter were performed within 10 min in 20 patients, followed by a fourth measure at the same location 6 h later. Intraclass coefficients were over 0.8 and Cronbach's alpha were over 0.9 for lumen diameter and WLR (see supplementary Table 1 Table 1, http://links.lww.com/HJH/A316). The threshold of significance was set to $P = 0.05$ for all tests. Pearson's correlation coefficient was calculated to estimate the linear relationship between two variables. Multiple regression (backward stepwise method) was carried out to identify predictors of WLR. All analyses were performed with SPSS software (version 19; IBM Corporation, Arbank, New York, USA).

## RESULTS

By adaptive optics imaging, the red cell column of arteries and veins appeared as dark stripes with an axial reflection. Along both sides of the blood column of arteries, a linear structure was visible (Fig. 1a). This structure was observed on individual video frames (supplementary videos 1 and 2, http://links.lww.com/HJH/A317, http://links.lww.com/HJH/A318[adaptive optics video fundoscopy of the superotemporal artery and vein in the right eye of a 26-year-old man (same patient as in figure 1). Note the visibility of the arterial wall but not of the venous wall, and the systolic curving of the arteriole (Quicktime video; image width 1.2 mm; 40 frames, 10 fps); adaptive optics video fundoscopy of the superotemporal artery in the right eye of a 40-year-old healthy woman (Quicktime video; image width 1.2 mm; 40 frames, 10 fps)]), hence ruling out a blurring artifact due to systolic expansion. Parietal

**TABLE 1. Clinical and morphometric characteristics of the study population (mean ±SD)**

| | Total | Normotensive | Hypertensive | P* |
|---|---|---|---|---|
| *n* | 49 (23F, 26M) | 30 (15F, 15M) | 19 (8F, 11M) | |
| Age (years) | 44.9 ± 14.4 | 42.3 ± 15 | 48 ± 11 | NS |
| BMI | 24.9 ± 4.7 | 23.8 ± 4.5 | 26.4 ± 4 | NS |
| SBP (mmHg) | 132.5 ± 22.2 | 118 ± 13 | 154 ± 14 | <0.01 |
| DBP (mmHg) | 82.6 ± 14 | 74 ± 9.5 | 95.5 ± 10 | <0.01 |
| Mean BP (mmHg) | 99 ± 16 | 88.8 ± 10 | 113.8 ± 11 | <0.01 |
| Pulse BP (mmHg) | 49.9 ± 12 | 43.7 ± 9 | 58.9 ± 11 | <0.01 |
| D (μm) | 79.8 ± 12 | 83.5 ± 11.2 | 74 ± 12.6 | <0.05 |
| P (μm) | 24.3 ± 3.7 | 23.5 ± 3.7 | 25.5 ± 3.3 | NS |
| WLR | 0.31 ± 0.07 | 0.285 ± 0.05 | 0.36 ± 0.08 | <0.01 |
| WCSA ($\mu m^2$) | 3411 ± 874 | 3459 ± 915 | 3338 ± 826 | NS |

BP, blood pressure; D, diameter; NS, not statistically significant; P, parietal thickness; WCSA, wall cross-sectional surface; WLR, wall-to-lumen ratio.
*Between normo and hypertensive.

structures were visible in arterioles as small as 25 μm. Their visibility did not depend on its orientation relative to the nerve fiber layer, ruling out an optical effect of ganglion cell axons.

## Correlation of arteriolar morphometry and blood pressure

Forty-nine normotensive or treatment-naive hypertensive individuals were included (Table 1). Nineteen had systolic pressure over 139 mmHg, while 30 were below. In hypertensive patients, the lumen diameter of the superotemporal artery was significantly lower, and the WLR was significantly higher. There was no significant difference of WCSA between groups. By univariate analysis, a number of significant correlations were found (Fig. 2 and Table 2). Multiple regression was carried out taking into account age, BMI, systolic, mean, and pulse pressure. The linear combination of these factors that gave the most accurate prediction of WLR was:

$$\mathrm{WLR} = 0.0051 + 0.0025 \times \text{mean pressure} + 0.0014 \times \text{age}$$

which accounted for 43% of the variability of WLR. This suggests that mean pressure had a stronger effect on WLR than age.

## Adaptive optics imaging of focal vascular changes

In a distinct cohort, adaptive optics images of arteriovenous crossings and FANs were analyzed. Classical concepts of the pathophysiology of AVNs postulate that venous nicking is due to mechanical compression from overlying arterioles. Alternatively, the implication of retinal cells was suggested by histology. In order to progress in the understanding of AVNs, adaptive optics images of 10 normal arteriovenous crossings from nine patients (age range, 26–62 years) were compared with adaptive optics images of 12 AVNs from 12 patients (age range, 47–77 years). In normal arteriovenous crossings (Fig. 3a), venules were seen crossing under the arteriole without notably changing their caliber or their pathway. The borders of the vein lumen remained clearly visible up to the area of arteriovenous overlap. In AVNs (Fig. 3b and c, and supplementary Figure 1, http://links.lww.com/HJH/A316), the vein appeared frequently blurred upstream and downstream. One or more sites of focal venous narrowing could be often seen upstream and/or downstream of the crossing site (asterisks in figures). The overlying arteriole did not show evidence of parietal thickening; The WLR was indeed not significantly different between AVNs and control areas (Fig. 3b). In order to better understand the arteriovenous relationship at sites of AVNs, we documented by adaptive optics four cases of venous nicking occurring at a site where an arteriole and a venule ran in parallel, yet without overlapping (Fig. 4c and supplementary Figure 2, bottom, http://links.lww.com/HJH/A316). This peculiar anatomical feature, which is clinically and histologically similar to AVNs with overlapping vessels [19] allowed a direct observation of the arteriovenous interface. In all cases, there was a gap 10–30 μm wide between the artery and the vein, suggesting that physical contact between the arteriole and the venule is not a prerequisite for venous nicking.

In 10 FANs from 10 patients (age range, 47–64 years), we observed that, in most cases, the inner and outer vascular limits remained parallel throughout the FAN (Fig. 4 and supplementary Figure 2, http://links.lww.com/HJH/A316), focal parietal thickening being detected in only two cases. Therefore, the WLR in FANs was locally increased, in relationship with the decrease of lumen diameter. Conversely, the WCSA was not increased, indicating that there was no significant parietal growth at sites of FANs. Taken together, this favors the hypothesis that focal vasoconstriction is involved in FANs.

# DISCUSSION

Here, we show that adaptive optics imaging allows qualitative and quantitative microvascular morphometry of small vessels at a near-histological scale, which allowed us to explore the structural basis of the various manifestations of hypertensive retinopathy. In a cohort of treatment-naive individuals, our data suggests that a higher BP is accompanied by parietal thickening and lumen narrowing, and hence increased WLR of retinal vessels. This supports the notion that a diffuse vasoconstriction accompanies BP increase. As the WLR is dimensionless, any bias due to refraction is neutralized, reinforcing the robustness of our findings. This transversal study cannot, however, determine

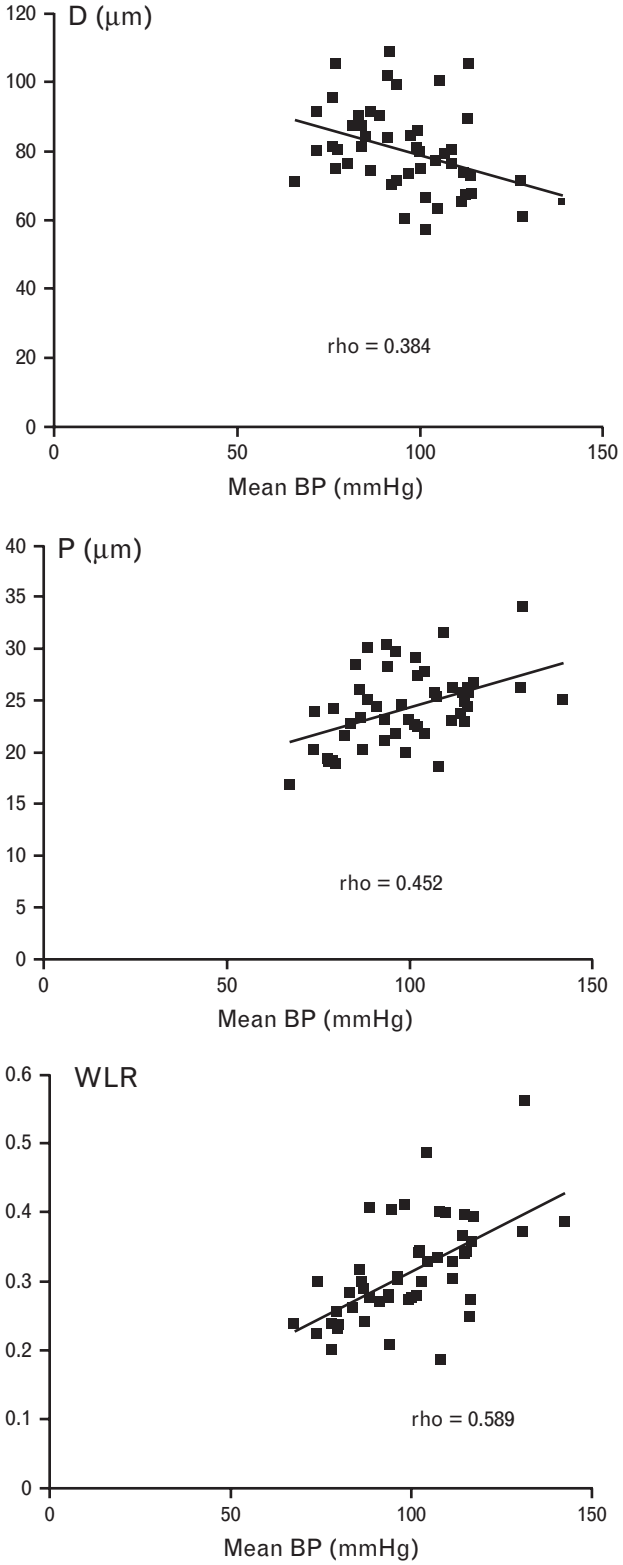


**FIGURE 2** Mean blood pressure plotted against parietal (P), diameter (D) and wall-to-lumen ratio (WLR). Pearson's correlation coefficients are inserted. All regressions lines are statistically significant ($P < 0.01$).

any cause–effect relationship between BP rise and vasoconstriction.

Fundus photograph-based studies [27] reported an age-related decline of arterial lumen diameter, which may be interpreted as indirect evidence of parietal thickening. We did observe an inverse correlation of age with WLR by univariate analysis, and multiple regression analysis confirmed the effect of age on WLR. Additional studies with larger cohorts are necessary to further document the relationship between parietal thickness and age. Nevertheless, the correlation of arterial diameters with age appears somewhat weaker than with BP.

Although it is commonly assumed that diffuse parietal thickening is initiated by a myogenic response, the pathogenesis of focal vascular changes remains uncertain. While most research and hence conceptual efforts on hypertensive microvasculopathy addressed to diffuse changes of parietal thickness, focal microvascular changes received little attention. They are indeed difficult to track by histology. Clinical studies based on fundus photographs have shown that the incidence of focal changes is correlated with age, blood pressure, and inflammation biomarkers [28]. Interestingly, it has been reported that there is a significant turnover of focal changes [29], suggesting that they are dynamic rather than degenerative processes. By adaptive optics, FANS and AVNs showed distinct anatomical features. Interestingly, neither FANs nor AVNs seemed to involve parietal growth as their primary cause. In AVNs, adaptive optics revealed a combination of loss of retinal transparency and presence of focal venous narrowings upstream and downstream of the arteriovenous crossing. Moreover, adaptive optics images of AVNs in which the arteriovenous interface could be observed showed that venous nicking could occur even in the absence of arteriovenous contact. This is in accordance with histology studies, which reports that, instead of arterial compression, changes affecting structures adjacent to the arteriovenous crossing such as axons, glial cells or the extracellular matrix may be found [30–32]. Taken together, adaptive optics and histology data argues against the prevalent model stating that the arteriole compresses the underlying vein, and instead support the hypothesis that venous nicking is mediated by retinal structures, hence implying a diffusible process. At sites of FANs, the inner and outer limits of the arteriolar wall maintained their parallelism and there was no evidence of parietal growth, suggesting that FANs were caused by focal vasoconstriction.

The morphometry of veins is gaining interest as it has been shown that venous diameter is predictive of morbidity and mortality [33,34]. The inner diameter of veins, but not the parietal thickness, can be measured with high precision by adaptive optics, which could help to determine the effect of blood pressure control on venous diameter. Adaptive optics is also of interest for the identification of focal venous narrowing at sites of AVNs, which are likely the site at which venous obstruction may occur. Hence, adaptive optics may provide insights into the factors triggering branch retinal vein occlusion, a common finding during hypertensive retinopathy.

Despite these promising results, they have to be considered as preliminary and hence a number of investigations remain to be done. We did not compare our data to ex-vivo measures by myography; nevertheless, our results on WLR measurement are very close to those observed by SDLF. This is shown in Table 3, which

**TABLE 2. Univariate correlations between clinical and morphometric parameters**

| | D | P | WLR | WCSA |
|---|---|---|---|---|
| Age | −0.173 | 0.331* | 0.348* | 0.183 |
| BMI | −0.254 | 0.241* | 0.342* | 0 |
| SBP | −0.384** | 0.438* | 0.582** | 0.13 |
| DBP | −0.362* | 0.437* | 0.559** | 0.06 |
| Mean BP | −0.385** | 0.453* | 0.589** | 0.05 |
| Pulse pressure | −0.275 | 0.283 | 0.406** | 0.01 |

D, diameter; P, parietal thickness; WCSA, wall cross-sectional area; WLR, wall-to-lumen ratio.
*$P < 0.05$.
**$P < 0.01$.

compares the demographic, clinical and morphometric characteristics of our report and of reference [16]. As SDLF measures are well correlated with myographic data [17], this suggests that the WLR measured by adaptive optics imaging is a valid surrogate of the actual WLR. A potential bias may have been the use of topical tropicamide in some eyes. To

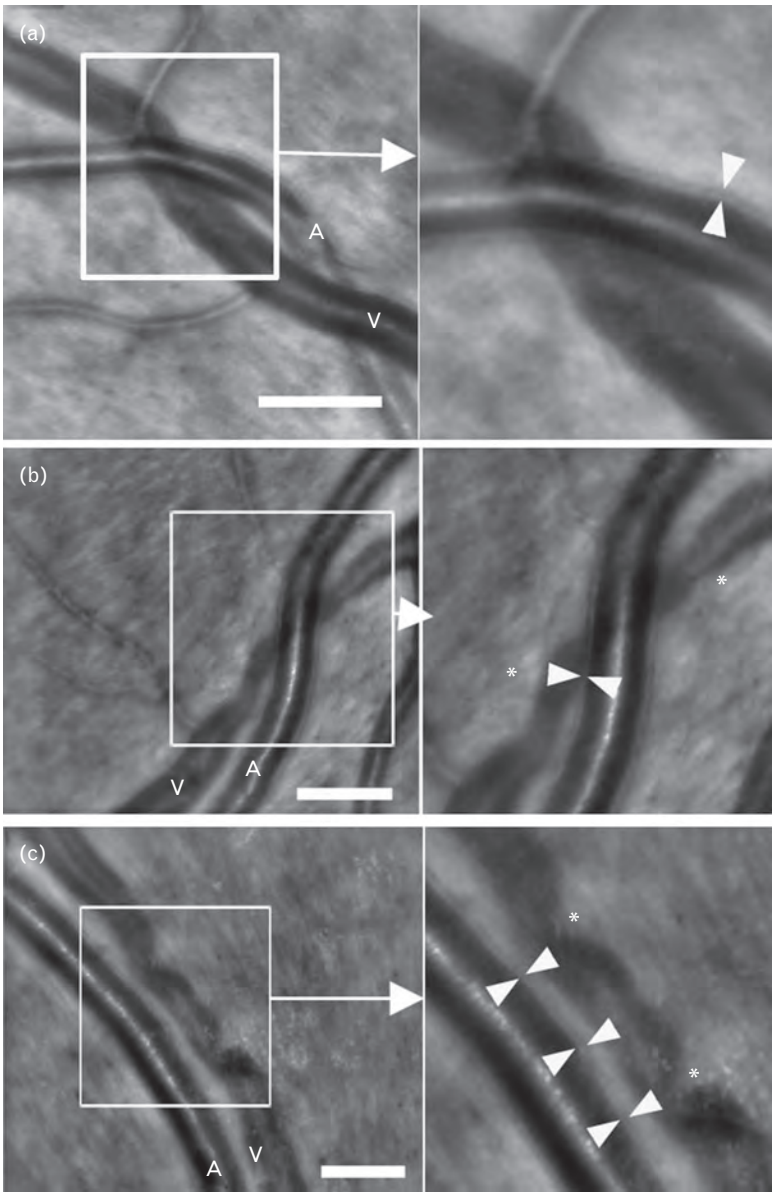


**FIGURE 3** Representative adaptive optics (AO) imaging of arteriovenous crossings. Arrowheads bracket the arteriolar wall. (a) Normal arteriovenous crossing (right panel: magnification). (b) Representative cases of arteriovenous nicking (AVN). Note the focal venous narrowings (asterisks) upstream and downstream of the arteriovenous overlap. (c) Case of venous nicking occurring in the immediate vicinity of an arteriole in the absence of arteriovenous overlapping, allowing the direct observation of the arteriovenous interface; note the gap between the arteriolar wall and the vein, suggesting that there is not direct contact (bars, 125 μm; additional cases are shown in supplementary Figure 1, http://links.lww.com/HJH/A316).

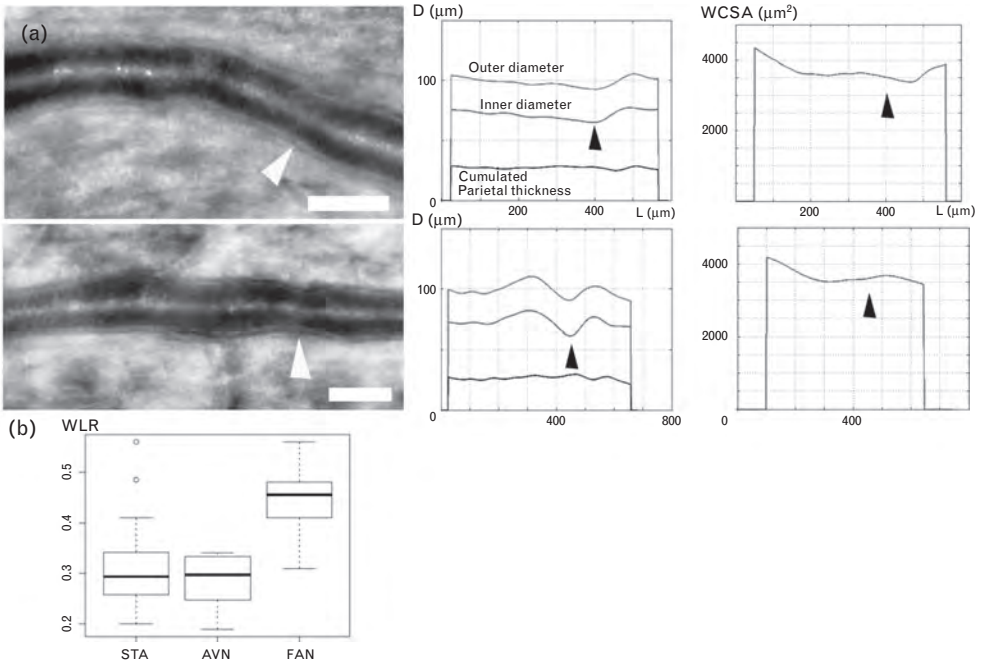


**FIGURE 4** (a) Adaptive optics (AO) NIR imaging of two representative cases of focal arteriolar narrowings (FANs) with their corresponding morphograms (arrowheads in AO images and in morphograms show lumen narrowing). In both cases, the parallelism of the inner and outer vascular limits was maintained. There was no detectable increase of WCSA at the site of FAN (bar, 100 μm; see also supplementary Figure 2, http://links.lww.com/HJH/A316). (b): comparison of wall-to-lumen ratio (WLR) between the superotemporal artery (STA), AVN ($n = 12$) and FANs ($n = 10$). The difference between groups is statistically significant ($P < 0.01$).

our knowledge, there is no report of the effect of topical tropicamide on major retinal vessels. In a series of nine eyes, we compared vascular morphometry before and after tropicamide administration. This showed that after tropicamide there was a mean increase of vascular diameter of 0.8%, which was not statistically significant (data not shown). We concluded that topical tropicamide had negligible effects in our measures.

A promising perspective of adaptive optics imaging is the follow-up of patients treated by antihypertensive drugs. There are indeed few reported studies of the effect of blood pressure control on retinal vascular morphometry [35,36] and on the effect of such modifications on the incidence of end-organ damage. It would be of high interest to determine if 'microvascular responders' (i.e. patients showing arteriolar vasodilation under treatment) have a better prognosis in term of end-organ damage. One can hypothesize that if there is no change in microvascular resistances, lowering blood pressure may hamper downstream perfusion. Also, the fact that AVNs may involve damage to adjacent neuroglial structures may also be of interest to understand the pathophysiology of age-related and hypertension-related brain damage given the functional similarities of retinal and cerebral vessels [37].

In conclusion, we show here that adaptive optics imaging of retinal arterioles offers a unique opportunity to explore microvascular changes *in vivo* in humans at a near-histology level, with a simple procedure applicable

**TABLE 3. Comparison of adaptive optics data from the present study and scanning laser Doppler flowmetry data from Ritt *et al.* [16]**

| | Present study | | Ritt 2008 | |
|---|---|---|---|---|
| | Normotensive | Hypertensive | Normotensive | Hypertensive |
| *n* | 30 | | 29 | |
| Age | 42.3 ± 15 | | 36.7 ± 5.9 | |
| Systolic pressure (mmHg) | 118 ± 13 | | 129 ± 6.9 | |
| Diastolic pressure (mmHg) | 74 ± 9.5 | | 77.8 ± 7.6 | |
| WLR | 0.285 ± 0.05 | | 0.28 ± 0.1 | |
| Lumen diameter (μm) | 83.5 ± 11.2 | | 85.3 ± 11 | |
| Wall cross-sectional area (μ²) | 3459 ± 915 | | 3740 ± 1415 | |
| *n* | | 19 | | 21 |
| Age | | 48 ± 11 | | 39.1 ± 5.4 |
| Systolic pressure (mmHg) | | 154 ± 14 | | 145 ± 6.8 |
| Diastolic pressure (mmHg) | | 95.5 ± 10 | | 87.7 ± 8.3 |
| WLR | | 0.36 ± 0.08 | | 0.36 ± 0.1 |
| Lumen diameter (μm) | | 74 ± 12.6 | | 81.8 ± 7.8 |
| Wall cross-sectional area (μ²) | | 3338 ± 826 | | 4413 ± 1725 |

in a routine setting. Quantitative and qualitative microvascular phenotyping by adaptive optics imaging may contribute to a better understanding of hypertensive retinopathy, and possibly improve medical management of small vessel diseases. Indeed, stratification of the risk of end-organ damage may be improved by biomarkers issued from adaptive optics imaging.

## ACKNOWLEDGEMENTS

ImagineEye provided technical assistance with image processing. We thank Dennis Han and Gabriel Quentel for helpful comments.

Supported by the Institut National de la Santé et de la Recherche Médicale (Contrat d'Interface 2011), the Agence Nationale de la Recherche (ANR-09-TECS-009 and ANR-12-TECS-0015–03) and the Association Contre l'OVR (www.asso-ovr.fr). The funding organizations had no role in the design or conduct of this research.

Registered in clinicaltrials.gov (NCT01546181).

### Conflicts of interest

M.P. is a consultant for the manufacturer of the camera used in the present study.

## REFERENCES

1. Heagerty AM, Aalkjaer C, Bund SJ, Korsgaard N, Mulvany MJ. Small artery structure in hypertension: dual processes of remodeling and growth. *Hypertension* 1993; 21:391–397.
2. Heagerty AM. Predicting hypertension complications from small artery structure. *J Hypertens* 2007; 25:939–940.
3. Buus NH, Mathiassen ON, Fenger-Grøn M, Præstholm MN, Sihm I, Thybo NK, *et al.* Small artery structure during antihypertensive therapy is an independent predictor of cardiovascular events in essential hypertension. *J Hypertens* 2013; 31:791–797.
4. Mulvany MJ. Small artery remodeling in hypertension. *Curr Hypertens Rep* 2002; 4:49–55.
5. Feihl F, Liaudet L, Levy BI, Waeber B. Hypertension and microvascular remodelling. *Cardiovasc Res* 2008; 78:274–278.
6. Martinez-Lemus LA, Hill MA, Meininger GA. The plastic nature of the vascular wall: a continuum of remodeling events contributing to control of arteriolar diameter and structure. *Physiology* 2009; 24:45–57.
7. Wong TY, Klein R, Klein BE, Meuer SM, Hubbard LD. Retinal vessel diameters and their associations with age and blood pressure. *Invest Ophthalmol Vis Sci* 2003; 44:4644–4650.
8. Wong TY, Klein R, Sharrett AR, Duncan BB, Couper DJ, Klein BE, *et al.* Atherosclerosis Risk in Communities Study. Retinal arteriolar diameter and risk for hypertension. *Ann Intern Med* 2004; 140:248–255.
9. Ikram MK, De Jong FJ, Vingerling JR, Witteman JC, Hofman A, Breteler MM, De Jong PT. Are retinal arteriolar or venular diameters associated with markers for cardiovascular disorders? The Rotterdam Study. *Invest Ophthalmol Vis Sci* 2004; 45:2129–2134.
10. Ikram MK, Witteman JC, Vingerling JR, Breteler MM, Hofman A, de Jong PT. Retinal vessel diameters and risk of hypertension: the Rotterdam Study. *Hypertension* 2006; 47:189–194.
11. Wong TY, Klein R, Nieto FJ, Klein BE, Sharrett AR, Meuer SM, *et al.* Retinal microvascular abnormalities and 10-year cardiovascular mortality: a population-based case-control study. *Ophthalmology* 2003; 110:933–940.
12. Haan M, Espeland MA, Klein BE, Casanova R, Gaussoin SA, Jackson RD, *et al.* Women's Health Initiative Memory Study and the Women's Health Initiative Sight Exam. Cognitive function and retinal and ischemic brain changes: the Women's Health Initiative. *Neurology* 2012; 78:942–949.
13. Lindley RI, Wang JJ, Wong MC, Mitchell P, Liew G, Hand P, *et al.* Multi-Centre Retina and Stroke Study (MCRS) Collaborative Group. Retinal microvasculature in acute lacunar stroke: a cross-sectional study. *Lancet Neurol* 2009; 8:628–634.
14. Yatsuya H, Folsom AR, Wong TY, Klein R, Klein BE, Sharrett AR. ARIC Study Investigators. Retinal microvascular abnormalities and risk of lacunar stroke: Atherosclerosis Risk in Communities Study. *Stroke* 2010; 41:1349–1355.
15. Harazny JM, Ritt M, Baleanu D, Ott C, Heckmann J, Schlaich MP, *et al.* Increased wall:lumen ratio of retinal arterioles in male patients with a history of a cerebrovascular event. *Hypertension* 2007; 50:623–629.
16. Ritt M, Harazny JM, Ott C, Schlaich MP, Schneider MP, Michelson G, Schmieder RE. Analysis of retinal arteriolar structure in never-treated patients with essential hypertension. *J Hypertens* 2008; 26:1427–1434.
17. Rizzoni D, Porteri E, Duse S, De Ciuceis C, Rosei CA, La Boria E, *et al.* Relationship between media-to-lumen ratio of subcutaneous small arteries and wall-to-lumen ratio of retinal arterioles evaluated non-invasively by scanning laser Doppler flowmetry. *J Hypertens* 2012; 30:1169–1175.
18. Liang J, Williams DR, Miller DT. Supernormal vision and high-resolution retinal imaging through adaptive optics. *J Opt Soc Am* 1997; 14:2884–2892.
19. Martin JA, Roorda A. Direct and noninvasive assessment of parafoveal capillary leukocyte velocity. *Ophthalmology* 2005; 112:2219–2224.
20. Chui TY, Vannasdale DA, Burns SA. The use of forward scatter to improve retinal vascular imaging with an adaptive optics scanning laser ophthalmoscope. *Biomed Opt Express* 2012; 10:2537–2549.
21. Rosenbaum D, Koch E, Girerd X, Rossant F, Paques M. Retinal arteries imaging by adaptive optics, feasibility and reproducibility. *Ann Cardiol Angeiol (Paris)* 2013; 62:184–188.
22. Gocho K, Sarda V, Falah S, Sahel JA, Sennlaub F, Benchaboune M, *et al.* Adaptive optics imaging of geographic atrophy. *Invest Ophthalmol Vis Sci* 2013; 54:3673–3680.
23. Weickert J, Romeny BH, Viergever M. Efficient and reliable schemes for nonlinear diffusion filtering. *IEEE Transac Image Process* 1998; 7:398–410.
24. Kass M, Witkin A, Terzopoulos D. Snakes: active contour models. *Int J Computer Vis* 1988; 1:321–331.
25. Xu C, Prince JL. Snakes, shapes, and gradient vector flow. *IEEE Trans Image Process* 1998; 7:359–369.
26. Ghorbel I, Rossant F, Bloch I, Paques M. Modeling a parallelism constraint in active contours. Application to the segmentation of eye vessels and retinal layers. *18th IEEE International Conference on Image Processing.* 2011, pp. 445–448.
27. Kawasaki R, Cheung N, Wang JJ, Klein R, Klein BE, Cotch MF, *et al.* Retinal vessel diameters and risk of hypertension: the Multiethnic Study of Atherosclerosis. *J Hypertens* 2009; 27:2386–2393.
28. Klein R, Sharrett AR, Klein BE, Chambless LE, Cooper LS, Hubbard LD, Evans G. Are retinal arteriolar abnormalities related to atherosclerosis? The Atherosclerosis Risk in Communities Study. *Arterioscler Thromb Vasc Biol* 2000; 20:1644–1650.
29. Liew G, Campbell S, Klein R, Klein BE, Sharrett AR, Cotch MF, *et al.* Ten-year longitudinal changes in retinal microvascular lesions. The Atherosclerosis Risk in Communities Study. *Ophthalmology* 2011; 118:1612–1618.
30. Seitz R. *The retinal vessels: comparative ophthalmoscopic and histologic studies on healthy and diseased eye.* Saint-Louis: Mosby; 1964; Translated by Frederick C and Blodi CV.
31. Kimura T, Mizota A, Fujimoto N, Tsuyama Y. Light and electron microscopic studies on human retinal blood vessels of patients with sclerosis and hypertension. *Int Ophthalmol* 2005; 4:151–158.
32. Jefferies P, Clemett R, Day T. An anatomical study of retinal arteriovenous crossings and their role in the pathogenesis of retinal branch vein occlusions. *Aust N Z J Ophthalmol* 1993; 21:213–217.
33. Wong TY, Islam FM, Klein R, Klein BE, Cotch MF, Castro C, *et al.* Retinal vascular caliber, cardiovascular risk factors, and inflammation: the multiethnic study of atherosclerosis (MESA). *Invest Ophthalmol Vis Sci* 2006; 47:2341–2350.
34. Ikram MK, de Jong FJ, Vingerling JR, Witteman JC, Hofman A, Breteler MM, de Jong PT. Are retinal arteriolar or venular diameters associated with markers for cardiovascular disorders? The Rotterdam Study. *Invest Ophthalmol Vis Sci* 2004; 45:2129–2134.
35. Thom S, Stettler C, Stanton A, Witt N, Tapp R, Chaturvedi N, *et al.* Differential effects of antihypertensive treatment on the retinal microcirculation: an anglo-scandinavian cardiac outcomes trial substudy. *Hypertension* 2009; 54:405–408.

36. Hughes AD, Stanton AV, Jabbar AS, Chapman N, Martinez-Perez ME, Thom SA. Effect of antihypertensive treatment on retinal microvascular changes in hypertension. *J Hypertens* 2008; 26:1703–1707.

37. Baker ML, Hand PJ, Liew G, Wong TY, Rochtchina E, Mitchell P, *et al.*, Multi-Centre Retinal Stroke Study Group. Retinal microvascular signs may provide clues to the underlying vasculopathy in patients with deep intracerebral hemorrhage. *Stroke* 2010; 41:618–623.

## Reviewers' Summary Evaluations

### Reviewer 1

Small artery/arteriolar remodeling is a hallmark of hypertensive microangiopathy. In particular, increased wall/lumen ratio of the microvascular wall is associated with cardiovascular disease and end-organ damage. In the present study by Koch *et al.* Adaptive Optics (AO)-based fundusphotography was used to study (micro)vascular remodeling in both naive and treated hypertensive patients. The strength of this technique is that microvascular remodeling now can be studied noninvasively, which facilitates longitudinal follow-up (e.g. of treatment effects). An important requisite, however, is that this technique first needs validation to histological analysis (e.g. from gluteal biopsies).

### Reviewer 2

The study proposes an innovative and promising method of evaluation of retinal small artery morphology, and provides evidence of an association between wall–lumen ratio (WLR) of retinal arterioles and blood pressure values. However, no validation of the method in respect to other available techniques is provided.

Adaptive optics should be directly compared with scanning laser Doppler flowmetry, or, even better, with the evaluation of the media-to-lumen ratio of subcutaneous small resistance arteries with micromyographic approaches, which represent, at present, the 'gold standard' and prognostically relevant approach to the evaluation of small artery morphology in human beings.